Subdomain-Specific Collapse of Denatured Staphylococcal Nuclease Revealed by Single Molecule Fluorescence Resonance Energy Transfer Measurements

Pengcheng Liu,[†,‡,¶] Xianglan Meng,[†,§] Peng Qu,[§] Xin Sheng Zhao,[*,§] and Chih-chen Wang[*,‡]

National Laboratory of Biomacromolecules, Institute of Biophysics, Chinese Academy of Sciences, 15 Datun Road, Beijing 100101, China, Graduate School of the Chinese Academy of Sciences, Beijing 100049, China, Beijing National Laboratory for Molecular Sciences, State Key Laboratory for Structural Chemistry of Unstable and Stable Species, and Department of Chemical Biology, College of Chemistry and Molecular Engineering, Peking University, Beijing 100871, China

Received: November 7, 2008; Revised Manuscript Received: June 23, 2009

By using single molecule fluorescence resonance energy transfer (smFRET), the equilibrium denaturation of staphylococcal nuclease (SNase) induced by guanidinium hydrochloride (GdmCl) has been investigated. We have characterized the collapse of the denatured chain and its relation to structure formation. Two mutants, K28C/H124C and K28C/K97C, were constructed and labeled for monitoring the behaviors of the global molecule and the β subdomain, respectively. For both the labeled mutants, only native and non-native conformations were observed, and the non-native conformations expanded with increasing GdmCl concentrations. The non-native chains of the two derivatives exhibited different changes of persistence length at higher GdmCl concentrations, suggesting a subdomain-specific collapse of the denatured state of SNase. This local chain specific collapse is likely to play a role in modulating the formation of early intermediate during protein folding.

Introduction

The most challenging and controversial area in protein folding concerns its early stages.[1] Numerous experimental and theoretical kinetic studies have shown that proteins refold via an initial collapse of the polypeptide within 100 μs of dilution of denaturant.[2−5] This collapse was also reported to occur at higher denaturant concentrations in equilibrium experiments.[6] The fundamental question that this chain collapse is a nonspecific random heteropolymer collapse or a specific process accompanied by forming some structures is poorly understood so far.[7] The difficulty arises from the lack of appropriate techniques to characterize the structures at three main levels of the collapsed state: secondary structure elements, local structures, and the outline of the global fold of the entire backbone.[8] Recently, using ultrafast small-angle X-ray scattering (SAXS) combined with circular dichroism spectroscopy, the question of whether the collapse and secondary structure elements occur concomitantly or sequentially has been extensively explored.[9−12] However, the specificity of chain collapse involving the formation of local structures was usually inferred indirectly from the features of the burst phase products in millisecond refolding kinetics, such as nonisotropic increase of multisite distances,[8,13−15] sigmoidal unfolding dependence on the denaturant concentrations,[16] and the exponential submillisecond kinetics.[17,18] The latter two have been reported not to be necessarily indicative of specific structure formation.[19−21] Therefore direct monitoring the local structure and global fold of the collapsed state is no doubt pivotal.

Recently developed multisite single molecule fluorescence resonance energy transfer (smFRET) is a powerful method to study the specific chain collapse involving the formation of local structures. smFRET has an inherent ability to separate subpopulations of the native and denatured states in heterogeneous mixtures at equilibrium and is of special significance to study the denatured state at low denaturant concentrations with most molecules at their native conformation.[22] It is particularly suitable for studying the chain collapse of small proteins with decreasing denaturant concentration.[23−35] By placing FRET dye pairs at various positions of the molecule, the chain collapse of *CspTm*, a two-state folding cold shock protein, was reported to be isotropic across the whole polypeptide chain, which agrees well with Gaussian chain model even under near-physiological conditions.[32] In order to explore whether this nonspecific chain collapse would also occur in proteins that refold through multiple intermediates, we employed staphylococcal nuclease (SNase), a 149-residue protein consisting of a *N*-terminal five-stranded β barrel subdomain and a C-terminal three α-helical α subdomain, as a model protein. Recently a kinetic experiment has demonstrated that the folding process of SNase commences with a cooperative collapse involving a major portion of the denatured chain within the dead time of measurement and a following early intermediate with a partially formed β subdomain and largely disordered α helical region.[36] Nevertheless, much debate on the folding mechanism of SNase remains. Does SNase fold in equilibrium via a variable two-state[37] or three-state mechanism?[38] Does specific chain collapse occur in the early stage of its refolding process initiated by perturbations?[7]

In the present work, we investigated the folding mechanism of SNase in equilibrium by using smFRET. The dye pairs were placed between the two subdomains and within the β subdomain to probe the distance distributions of the global and the local chains and their dependence on denaturant concentrations. The data demonstrated that SNase adopted denaturation transition

* To whom correspondence should be addressed. E-mail: chihwang@sun5.ibp.ac.cn (C.C.W.); zhaoxs@pku.edu.cn (X.S.Z.).
† These authors contributed equally to this work.
‡ Institute of Biophysics, Chinese Academy of Sciences.
§ Peking University.
¶ Graduate School of the Chinese Academy of Sciences.

10.1021/jp809825x CCC: $40.75
Published on Web 08/13/2009

in guanidinium hydrochloride (GdmCl) from a fixed native state to variable non-native states in terms of the measured distances and the denatured state exhibited a subdomain-specific collapse with the decrease of GdmCl concentration. Since the specific-collapsed local chain corresponds to the structural portion in early kinetic intermediate, we inferred that this specific collapse of the denatured state may modulate the formation of an early intermediate in the multistate folding process of the protein.

Materials and Methods

Protein Preparation, Labeling, and Characterization. The plasmid pET-28a containing a C-terminal histidine-tagged SNase sequence was a kind gift of Prof. Guozhong Jing (Institute of Biophysics, CAS). Two cysteine mutants, K28C/K97C and K28C/H124C, were generated by site-directed mutagenesis taking pET-28a-SNase as a template to provide functional groups for specific fluorescence labeling. Wild-type SNase and K28C/H124C expressed in BL21 (DE3) and K28C/K97C in BL21 (DE3) pLysS were purified by a Chelating-Sepharose Fast Flow column (Amershan-Phamacia Biotech). The SNase elutes were lyophilized. The mutant elutes were dialyzed against 20 mM Tris-HCl containing 0.1 M NaCl and 30 mM 2-mercaptoethanol (pH 7.4) and stored at aliquots with 5% glycerol at −20 °C. Protein preparations were used within two weeks. Protein concentration was determined spectrophotometrically at 280 nm with an extinction coefficient of 0.93 mL mg^{-1} cm^{-1}.[39] Enzyme activity was assayed as described by Zhang.[40] Circular dichroism spectra were measured over the range 200−260 nm in a Pistar-180 spectrometer (Applied Photophysics, UK).

The thawed mutant proteins were reduced with 100-fold molar excess of Dithiothreitol (DTT) at 37 °C for 20 min followed by chromatography in labeling buffer (100 mM NaPi, pH 7.0, with 0.5 M NaCl and 2 mM Ethylene diamine tetraacetic acid (EDTA)) to remove the excess DTT and determined to be fully reduced by 5,5′-Dithiobis(2-nitrobenzoic Acid) (DTNB).[41] Site-specific labeling of the reduced mutants was achieved by reaction with thiol-reactive fluorescence dyes (Molecular Probes, Eugene, OR). A 1.5-fold molar excess of acceptor dye Alexa Fluor 647 C2-maleimide was added dropwise to 30−50 μM protein in labeling buffer for reaction of 2 h for K28C/H124C or 5−30 min for K28C/K97C and, then, incubated for further 2 h with 1.5-fold molar excess of donor dye Alexa Fluor 555 C2-maleimide. The two steps of reaction were carried out at room temperature in the dark with stirring followed by standing at 4 °C overnight. Unconjugated dyes were removed through a Sephadex G 25 column in buffer A (20 mM Tris-HCl containing 0.1 M NaCl, pH 7.6), and the labeled protein solution was concentrated and stored at −80 °C with 10% glycerol. Most of the labeled preparations were assessed to be double-labeled by absorbance measurement at 280 nm for protein, 555 nm for Alexa Fluor 555, and 650 nm for Alexa Fluor 647 using the extinction coefficients provided by the manufacturer and matrix-assisted laser desorption ionization time of flight (MALDI-TOF) mass spectrometry.

Equilibrium Denaturation Monitored by Ensemble Fluorescence. Wild-type and unlabeled mutant proteins at 1 μM were denatured in buffer B (buffer A with 10 mM $CaCl_2$) containing various concentrations of GdmCl at 25 °C for 20 h to reach equilibrium, and intrinsic fluorescence spectra between 305 and 400 nm excited at 295 nm were measured on a Shimadzu RF-5301 PC spectrofluorometer. The concentrations of GdmCl were determined by refractive-index.[42] Corresponding fluorescence spectra of the labeled mutant proteins at 0.01 μM in buffer B containing 1 μM SNase and various concentrations of GdmCl were recorded between 520 and 750 nm on a Renishaw1000 microscopic spectrometer (Britain) with a 514 nm argon ion laser (Melles Griot, USA). The denatured curves were fitted to a two-state model equation.[43]

Single Molecule Measurements and Data Reduction. Single molecule fluorescence measurements were carried out on a home-built dual-channel confocal fluorescence microscope equipped with 532-nm laser as an excitation source. The laser beam was focused inside the sample solution, through an oil immersion objective (NA 1.4, 100×, Nikon), 10 μm above the glass surface. Sample fluorescence was collected by the same objective. Passing through a 50-μm-diameter pinhole in the image plane of the objective, the collected fluorescence was separated into donor and acceptor components with a dichroic mirror (FF593-Di02, Semrock) and two final filter sets (Semrock LP03-532RU and Daheng 650-1100 nm holophote for the donor channel; Semrock LP01-633RU and Semrock FF01-692/40 for the acceptor channel). Each component was focused by an achromatic lens onto a photon-counting Avalanche Photodiode (APD) (Perkin-Elmer Optoelectronics SPCM-AQR-15). The output of signals collected by the two detectors was recorded in 6.4 μs bin time by a computer implemented correlator (Flex02-12D).

The samples for single molecule experiments were prepared by diluting labeled proteins to 100 pM in buffer B with varying concentrations (0−4 M, every 0.1 M between 0 and 1, 1.2, 1.5, 2, and 4 M) of GdmCl and 1 μM SNase, the presence of which was to reduce surface adsorption of the labeled proteins. About 40 μL sample solution was sealed between a chamber cover (Grace Bio) and a cover glass, which has been carefully cleaned in a piranha solution (30% H_2O_2: H_2SO_4 = 7:3 v/v) for more than 30 min at above 90 °C. All experiments were conducted at room temperature.

Fluorescence bursts of the 640 μs bin were taken to be significant when the sum of counts in the donor (n_D) and acceptor channels (n_A) was higher than a set threshold, and the smFRET histograms were built accordingly and further fitted by combination of a beta function for the native state and a Gaussian function for the non-native state. With the presence of both native and non-native peaks, the overlap between two peaks results in higher errors of the mean energy transfer efficiency for the non-native subpopulation. In order to validate these values, we fixed the fitting parameters for the native subpopulation as those obtained from the native peak at 0 M GdmCl, and only adjusted the amplitude to get the best parameters for the non-native peak.

Raw data were corrected for the following factors. (a) The background was calculated by fitting the low-count tail of raw photon counting histograms using Poisson distributions, which resulted in a larger but more accurate value than that obtained from the blank control solutions.[44] (b) Crosstalk between two channels was estimated by the emission spectrum of the donor and acceptor at two channels, and the leakages for both were less than 3%. (c) The relative quantum yields of Alexa Fluor 555-SNase and Alexa Fluor 647-SNase in different concentrations of GdmCl were measured according to Vámosi,[45] and the changes with denaturant concentrations were taken into account in the following calculation. (d) The ratio of collection efficiencies of two channels were determined by measuring signals of 10^{-7} M rhodamine 6G in two channels, which was verified by calculation using the known or measured parameters of the optical components.[29] (e) The contribution of direct excitation of the acceptor was estimated by the reported method.[32]

By measuring the donor quantum yield, the refractive index of the bulk solvent, and the overlap between the emission

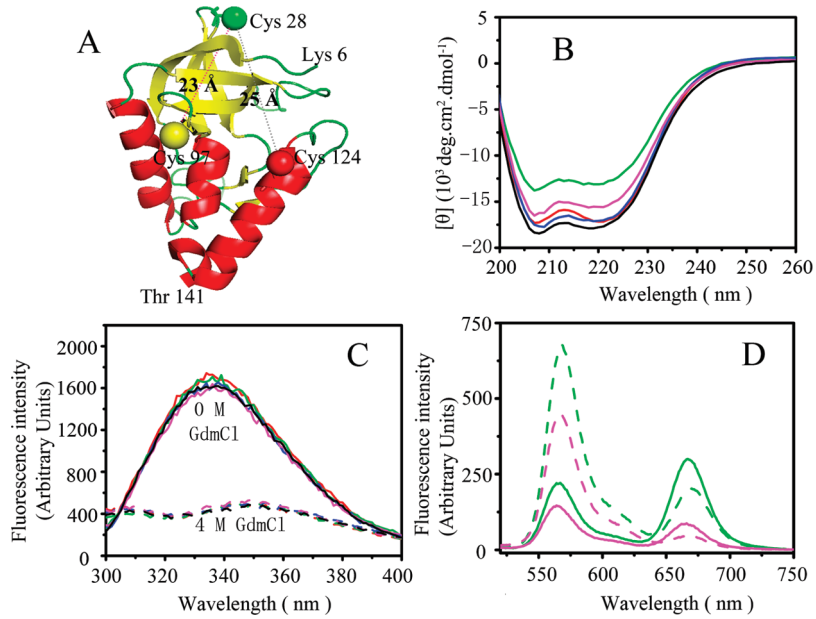

Figure 1. Characterization of SNase derivatives; cartoon representation (A) of SNase structure (PDB 1EY0) with K28 and K97 in subdomain β (yellow) and H124 in α (red) substituted by cysteine for fluorescence labeling. The distance between the two S atoms (balls) was estimated by using PyMOL (DeLano Scientific LLC, USA) to be 23 Å in K28C/K97C and 25 Å in K28C/H124C, respectively. Far-UV CD spectra of native SNase proteins (B) at 8 μM were measured in a 0.1 mm path-length cuvette at 25 °C. Intrinsic fluorescence spectra with excitation at 280 nm of SNase proteins (C) at 5 μM and fluorescence emission spectra with excitation at 500 nm of labeled proteins (D) at 0.1 μM in buffer B containing 1 μM wild-type SNase were measured after incubation at 25 °C for 20 h in the absence (solid curves) or presence (dashed curves) of 4 M GdmCl. Black, red, green, blue, and magenta curves denote the spectra of wild-type SNase, K28C/K97C, labeled K28C/K97C, K28C/H124C, and labeled K28C/H124C, respectively.

spectrum of the donor and the absorption spectrum of the acceptor, assuming freely rotating dyes (Alexa moieties with $\kappa^2 = 2/3$) for their long linkers and the surface-locating labeling sites, the Förster radius R_0 of the FRET dye pair at different GdmCl concentrations was estimated (Figure S1 of the Supporting Information).

Results

Construction of SNase Mutants. Two mutants K28C/K97C and K28C/H124C were constructed to characterize the size properties of the subdomain and global molecule in denatured states, respectively. As shown in Figure 1A C28 and C97 are located in the β subdomain while C124 is in α; they are all solvent-exposed with the distance between the two bound chromophores in both mutants being within the Förster radius R_0. The mutation and further labeling did not significantly change the shape of the far-UV circular dichroism (CD) spectra under native conditions, all of which showed broad negative bands with two minima at 206 and 222 nm, but the labeled derivatives exhibited a little decrease in the $[\theta]_{222nm}$ value (Figure 1B). SNase contains one tryptophan residue (W140) buried in a local hydrophobic environment of the C-terminus and seven tyrosine residues dispersed throughout the molecule. The native mutants and derivatives also showed very similar intrinsic fluorescence spectra with the same emission maximum of 338 nm when they were excited at 280 nm (Figure 1C) and contained at least 90% enzyme activity (data not shown) to that of the wild-type molecule. In the presence of 4 M GdmCl, these molecules showed a similar decrease in the fluorescence intensity and a substantial red shift of the emission maximum to 355 nm. Both the native and denatured double-labeled derivatives with donor and acceptor displayed significant FRET (Figure 1D), while the separate and mixed derivatives with donor only or acceptor only exhibited no FRET, suggesting little or no aggregation.

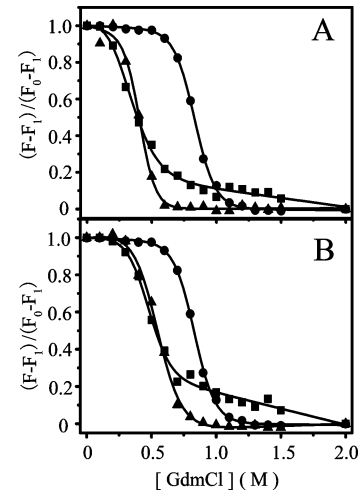

Figure 2. Equilibrium denaturation of SNase proteins. Denaturation curves of wild-type SNase (●) and nonlabeled (▲) K28C/K97C (A) or K28C/H124C (B) were determined by the changes of fluorescence intensity at 335 nm with excitation at 295 nm. The denaturation of labeled proteins (■) was followed by the changes of the emission intensity of donor dye at 565 nm. The data were fitted to a two-state folding model (solid curves) according to the work of Santoro and Bolen.[43] All the data were normalized as $(F - F_1)/(F_0 - F_1)$. F was determined at the indicated GdmCl concentration; F_0 and F_1 were determined for the native and fully denatured (with 2 M GdmCl) proteins, respectively.

Ensemble Equilibrium Denaturation of SNase Proteins. The fluorescence changes of W140 reflect the tertiary structure changes of SNase molecules.[46] As shown in Figure 2, the intrinsic fluorescence intensity at 335 nm with excitation at 295 nm of unlabeled SNase proteins in GdmCl-induced denaturation showed a two-state transition with the thermodynamic parameters in Table 1. The ensemble FRET of labeled SNase mutants exhibited a donor emission increase and an accompanying

TABLE 1: Thermodynamic Parameters for GdmCl-Induced Denaturation of SNase Proteins[a]

		ΔG^0 (kcal mol^{-1})	m_G (kcal mol^{-1} M^{-1})	$C_{1/2}$ (M)
SNase	intrinsic flu[b]	6.1	7.3	0.84
K28C/K97C	intrinsic flu[b]	3.7	9.0	0.42
	donor flu	1.5	5.4	0.28
K28C/H124C	intrinsic flu[b]	3.2	5.8	0.56
	Donor Flu	3.2	7.0	0.47

[a] All the data were averages of at least two independent experiments. [b] For unlabeled proteins.

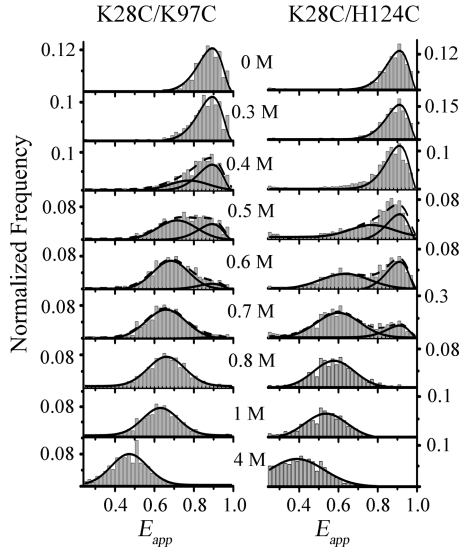

Figure 3. Histograms of energy transfer efficiency from smFRET measurements. Curves are the best fit to folded and unfolded subpopulations using beta and/or Gaussian functions, respectively.

acceptor emission decrease with increasing the GdmCl concentration from 0 to 2 M (data not shown). The denaturation curves of the labeled proteins (Figure 2), with the folded fractions determined by the changes of the emission intensity of the donor dye at 565 nm, were fitted to a two-state model but with apparently influence on the stability (Table 1), indicating some interference of fluorophore labeling on SNase equilibrium denaturation.

smFRET Measurements of SNase Denaturation. When single protein molecules labeled with both donor and acceptor diffused freely through the focal volume of the laser beam, the donor was excited and energy was transferred to the acceptor at different extents corresponding to different FRET efficiencies. For each event, the apparent mean FRET efficiency $\langle E_{app}\rangle$ was calculated by $\langle E_{app}\rangle = n_A/(n_A + n_D)$, where n_A and n_D were the number of collected photons of acceptor and donor, respectively. As shown in Figure 3, histograms of both derivatives at low concentrations of GdmCl showed one peak with high FRET efficiency (centered at 0.91 for K28C/H124C and 0.89 for K28C/K97C), which was assigned to the native state. With increasing concentrations of GdmCl, one more peak appeared with mediate FRET efficiency and increased its amplitude relative to the native peak, corresponding to the non-native state. Above 0.8 M GdmCl, only the non-native peak remained. The peak at $E_{app} \approx 0$ was a ubiquitous artifact, which arose from the molecules without active acceptor or the impurities in solution and was omitted in the histograms.[25,29,31,32] $\langle E_{app}\rangle$ of the native state was invariant in different GdmCl concentrations, but $\langle E_{app}\rangle$ of the non-native state continuously decreased with increasing the GdmCl concentrations, suggesting a collapse of the denatured chain.

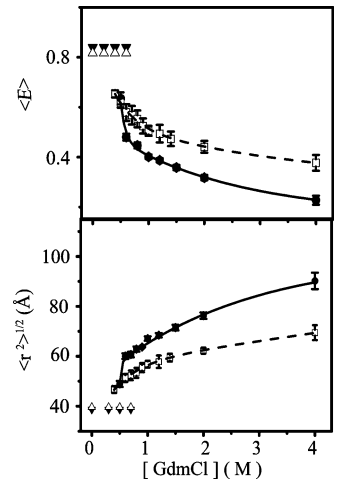

Figure 4. Dependence of the corrected FRET efficiency $\langle E\rangle$ and the chain dimensions of SNase on the GdmCl concentrations. (A) Mean FRET efficiencies $\langle E\rangle$ for the native states (▼ for K28C/H124C and Δ for K28C/K97C) and the denatured state (● for K28C/H124C and □ for K28C/K97C). (B) Root-mean-square end-to-end distances ($\langle r^2\rangle^{1/2}$) in the native (▼ for K28C/H124C and Δ for K28C/K97C) and the denatured (● for K28C/H124C and □ for K28C/K97C) mutants were calculated from the data in part A with a static Förster function and Gaussian chain approximation, respectively.

Distance Calculation from Accurate Mean Transfer Efficiencies. In order to calculate the average interdye distance, $\langle E_{app}\rangle$ must be corrected for several factors mentioned in *materials and methods* to get accurate mean transfer efficiency $\langle E\rangle$. The results were shown in Figure 4A.

The FRET efficiency distribution of the denatured state does not directly provide the distribution of the end-to-end distance. Considering that the fluctuation dynamics of the denatured peptide chains was on the time range from nanoseconds to dozens of microseconds,[30,47−49] the averaging of the conformational fluctuations would occur within the burst time in our experiments. Hence, we took the mean energy transfer efficiency of the unfolded state as an average over the end-to-end distance distribution, $P(r)$, and adopted the Gaussian chain model for the probability distribution of the end-to-end distance. Thus, the mean transfer efficiency was expressed according to[32]

$$\langle E\rangle = \int_0^L E(r)P(r)\,dr \Big/ \int_0^L P(r)\,dr \qquad (1)$$

with the distance dependence of the FRET:

$$E(r) = \frac{1}{1 + \left(\frac{r}{R_0}\right)^6} \qquad (2)$$

and the end-to-end distance probability density function of a Gaussian chain:

$$P(r) = 4\pi r^2 \left(\frac{3}{2\pi\langle r^2\rangle}\right)^{2/3} \exp\left(-\frac{3r^2}{2\langle r^2\rangle}\right) \qquad (3)$$

here, r is the end-to-end distance, L is the contour length, and R_0 is the Förster radius of the FRET pair.

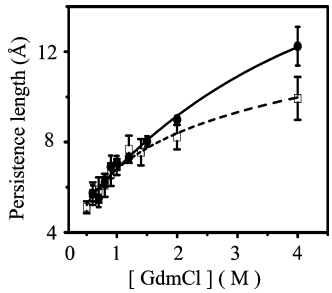

Figure 5. Denaturant dependence of persistence length l_p. Lines are the best fit of l_p for K28C/K97C (□) and K28C/H124C (●). The data are the averages of three individual experiments.

The root-mean-square end-to-end distance $\langle r^2\rangle^{1/2}$ of the two derivatives (Figure 4B) were calculated from experimentally determined $\langle E\rangle$. It was obvious that the denatured state of SNase underwent a continuous collapse with the decrease of GdmCl concentration. Strikingly, an abrupt decrease of $\langle r^2\rangle^{1/2}$ was observed for K28C/H124C at 0.5 M GdmCl, while it was not seen for K28C/K97C. Considering the unusual decrease, we extrapolate the $\langle r^2\rangle^{1/2}$ above 0.6 M for K28C/H124C, with the result of 50 Å at 0 M GdmCl, and 36 Å was derived for K28C/K97C with all of the concentrations considered. The extrapolated value for K28C/H124C was a little higher than the respective $\langle r^2\rangle^{1/2}$ of the native state calculated directly from the experimentally determined $\langle E\rangle$ (37 Å for K28C/H124C and 38 Å for K28C/K97C), differing from that of K28C/K97C which is close to the native value. Also, in the same way, the R_g of the non-native state extrapolated to native condition is 24 Å for K28C/K97C and 21 Å for K28C/H124C, which are both larger than 15.6 Å for the folded state reported by SAXS.[50] In the calculation of R_g, dye-linkers were considered to be equivalent to an additional 6 amino acid residues, and the Gaussian chain model according to Flory scaling law,[51] $R_g = [149/(n + 6)]^{1/2}(\langle r^2\rangle/6)^{1/2}$, was applied.

Persistence Length of the Two Derivatives. We also calculated the persistence length (l_p) of the denatured polypeptide chain for the two derivatives. In general, taking a Gaussian chain (long flexible chain with $L \gg l_p$) as a model for the denatured polypeptide chain, the correlation of persistence length and the mean square end-to-end distance $\langle r^2\rangle$ can be expressed as

$$\langle r^2\rangle = 2l_p l_c = 2l_p nl \qquad (4)$$

where n is the number of peptide bonds between the donor and acceptor dyes and l is the projection of the distance between two consecutive α-carbon atoms on the axis of the fully extended chain, 3.8 Å.[32] As shown in Figure 5, the value of l_p at 4 M GdmCl was 12 Å for K28C/H124C and 10 Å for K28C/K97C, and both decreased with decreasing GdmCl concentration to almost the same values between 0.6 and 1 M GdmCl.

Discussion

Although previous kinetic experiments have indicated that SNase folds to the native state via several partially structured intermediates populated along two or more parallel pathways,[36] the interpretation of SNase folding in equilibrium has been highly controversial for a long time.[52] Shortle proposed that SNase undergoes a two-state denaturation induced by GdmCl with different denatured ensembles in terms of the surface area exposed to denaturant.[37] Differently, based largely on thermal denaturation data, Carri and Privalov described the denaturation of SNase by a three-state model including a distinct intermediate.[38] The critical point for the two different views is to distinguish a "compact denatured ensemble" maintaining residual structures from a "discrete intermediate state" existing between the fully denatured and the native state at low GdmCl concentrations. This low denaturant regime is very difficult to access by traditional ensemble equilibrium experiments, because the ensemble signal is dominated by a large population of the native molecules. smFRET measurements are thought to enable us to observe single molecules and resolve the low populated subpopulations and, therefore, ensure characterization of the non-native state of SNase in the presence of an excess of native molecules. By using smFRET measurement, we observed only one constant and one shifting subpopulation distribution during the equilibrium denaturation of SNase induced by GdmCl. The widths of FRET efficiency distributions corresponding to the non-native states, which usually provide information about heterogeneities of proteins, exhibit same values within the experimental error (Figure S3 of the Supporting Information). It seems that single molecule measurements provide direct evidence for the two-state SNase folding. However, it should be noted that single molecule measurements can hardly distinguish subpopulations if they have very close peak positions, fast kinetic exchange, or small populations. In fact, we observed an abrupt decrease of interdye distance for the non-native states of K28C/H124C in low concentrations of GdmCl (0.5 and 0.6 M), suggesting the existence of an intermediate with a smaller interdye distance under mildly denaturing conditions. With the increase of GdmCl concentration, $\langle E\rangle$ of the non-native state of SNase exhibited a gradual decrease, indicating the expansion of the denatured state. Hence, our results of single molecule measurements showed that the equilibrium denaturation of SNase populated at least variable denatured states, the native state, and the possible intermediate, which agrees with recently reported kinetic results.[50]

The global sizes of denatured states under highly denaturing conditions are expected to agree with Gaussian chain statistics as "random coil" polymers.[53] The gyration radius R_g follows a simple scaling law proposed first by Flory and Tanford.[54] The values of R_g determined in 4 M GdmCl in our experiments, 42 ± 1 Å for K28C/K97C and 44 ± 3 Å for K28C/H124C, are close to the 45 Å expected for the random coil polymer with the same chain length,[55] but larger than the 37.2 ± 2.4 Å measured in 6 M GdmCl by using SAXS.[53]

Both the sizes of the local segment and the global molecule of the denatured chain were severely reduced with the decrease of GdmCl concentration. Different from that for K28C/K97C, the average interdye distance for K28C/H124C decreased abruptly from 0.6 to 0.5 M GdmCl, suggesting that large conformational changes for the globule molecules at 0.5 to 0.6 M GdmCl possibly lead to the formation of the intermediate.

To distinguish the collapse behaviors of the two derivatives, we compared the dependence of persistence length on GdmCl concentrations. This parameter, with a concomitant renormalization for chain length, enables a direct comparison of the derivatives with different sequence separation of the donor and acceptor.[32] Our analysis demonstrated that the two derivatives exhibited unambiguously different changes of persistence length at higher GdmCl concentrations. The differences unlikely arise from different photophysical properties of the dyes at different positions of the molecule, because the interaction between the protein molecule and the attached chromophores would be shielded under high concentrations of GdmCl,[31] and the fluorescence polarization measurements showed little influence of

GdmCl-induced SNase denaturation on the anisotropy values of labeled dyes (Figure S1A of the Supporting Information). It also does not arise from structure changes of the denatured SNase due to mutation,[56] as the influence of mutation was only exerted in a narrow range of low GdmCl concentrations. Therefore, the observed different GdmCl dependence of persistence length between the two derivatives can only represent real different collapse behaviors of the local chain and the global molecule of SNase.

The different persistence length for K28C/H124C and K28C/K97C at high concentrations of GdmCl (at 4 M in our experiments) suggested that the denatured state of SNase kept a significant amount of residual structures, since an intrinsically flexible chain without interactions to stabilize a specific structure adopts a fixed persistence length and is independent of the chain length.[57] In line with this conclusion, the denatured SNase in 8 M urea was reported to exhibit residual long-range order similar to the native topology,[58] and simulation also suggested that even a denatured "random coil" protein may contain segments of native structure linked with flexible chains.[59] The lower persistence length for K28C/K97C thus might result from more residual structures in the β subdomain compared with the rest of the molecule. As a matter of fact, it has been reported that the most stable interactions of the denatured state are within the β subdomain.[60] It is conceivable that more residual structures in the β subdomain at high concentrations of GdmCl will lead to less increase of residual structures than that of the remaining portion of the global molecule when transferred to lower GdmCl. This may be the reason why the decrease of persistence length for K28C/K97C is not as dramatic as K28C/H124C with the decrease of GdmCl concentrations. In mildly denaturing conditions, the almost similar changes of persistence length on GdmCl concentration seemingly suggest the same evolution of residual structures in different parts of the molecule. However, it should be noticed that other effects, photophysical properties of the dyes and the formation of static structures, may also perturb the determination of persistence length under weak denaturing conditions. Hence, the different dependence of persistence length on GdmCl concentration under harsh denaturing conditions provided a strong indication of the subdomain-specific collapse of the denatured SNase.

The molecular forces driving the denatured chain collapse probably result from hydrophobic interactions as well as the formation of intrachain hydrogen bonds.[34] In the β subdomain, several buried hydrophobic residues form a hydrophobic core of the molecule through the extensive interaction network.[61] Our observation that the β subdomain has more residual structures implies that hydrophobic interactions make major contributions to denatured chain collapse. This speculation was bolstered by the observation that hydrophobic collapse preceded the formation of substantial secondary structure in the folding process of SNase.[62] Recent reports have shown that native structure is a key determinant of the folding trajectory in the 2D conformational space defined by secondary structural content and R_g, while the stability of individual elements of secondary structure can also influence this folding trajectory.[63] It is reasonable to infer that denatured proteins of the α/β class and the all-β class exhibit different behaviors of chain collapse. This hypothesis could explain the different collapse behaviors of SNase, a α/β class protein, and *CspTm*, an all-β small protein.[32]

Conformational properties of the denatured protein would play a significant role in the refolding kinetics, particularly in the early steps of folding. It has been speculated that the impact of chain collapse on concomitant or subsequent folding of proteins might depend on the nature of the collapse.[12] However, it is difficult to dissect the nonspecific and specific components of the chain collapse in the early stage of protein folding. Denatured *CspTm* exhibits a nonspecific collapse across the whole polypeptide chain in equilibrium experiments.[32] Meanwhile, the chain collapse of barstar in the burst phase of kinetic experiments is gradual transformations of nonspecific global contraction from a completely denatured to a denatured molecule under refolding conditions and subsequently specific contraction in limited parts of the molecule to a refolding intermediate.[13] Our work on SNase also demonstrated that a specific collapse occurred in the hydrophobic core of the β subdomain even at higher concentrations of GdmCl where only the denatured state exists at equilibrium. This result showed that the specific collapse of denatured states could occur even under harsh denaturing conditions, while previous kinetics experiments showed that the specific collapse accompanies the formation of early intermediates.[9,13] Since kinetic experiments have shown the presence of an early intermediate with a stable β subdomain and a largely disordered α-helical region,[36] we infer that the specific collapse of a denatured chain might accelerate the formation of the early intermediate by limiting the conformational space of the local chain. Our results thus provide new insights into the importance of preorganized nonrandom structures in the denatured state to modulating the formation of the intermediate in the multistate folding process of proteins.

Conclusion

Using diffusion smFRET, we have shown that GdmCl-induced denaturation of SNase is a transition with a size-constant native conformation and variable non-native conformations. The denatured molecules become gradually expansionary with the increase of GdmCl concentrations, indicating a collapse of denatured molecules at lower concentrations of GdmCl. Further comparison of the denaturant-induced conformational changes between the β subdomain and the global molecule demonstrated a subdomain-specific collapse of denatured SNase. This collapse will populate more residual structures in the β subdomain, the region corresponding to the portion containing structures in an early folding intermediate, suggesting that the residual structures populated in denatured states would help to direct searching for conformational space in the early folding stages. Using ultrafast mixing techniques to further explore the relationships between the chain collapse and the formation of early intermediates is now under way.

Acknowledgment. This work was supported by the grants 20673002, 20733001, and 30620130109 from the Chinese Natural Science Foundation and 2006CB910903, 2006CB910304, and 2006CB806508 from the Chinese Ministry of Science and Technology. We thank Prof. Guozhong Jing for his generous gift of the pET-28a-SNase.

Supporting Information Available: Estimation of the Förster radius and ensemble FRET measurement. This material is available free of charge via the Internet at http://pubs.acs.org.

References and Notes

(1) Religa, T. L.; Markson, J. S.; Mayor, U.; Freund, S. M. V.; Fersht, A. R. *Nature* **2005**, *437*, 1053.
(2) Ballew, R. M.; Sabelko, J.; Gruebele, M. *Proc. Natl. Acad. Sci. U.S.A.* **1996**, *93*, 5759.
(3) Shastry, M. C. R.; Roder, H. *Nat. Struct. Biol.* **1998**, *5*, 385.
(4) Lapidus, L. J.; Yao, S. H.; McGarrity, K. S.; Hertzog, D. E.; Tubman, E.; Bakajin, O. *Biophys. J.* **2007**, *93*, 218.

(5) Onuchic, J. N.; Luthey-Schulten, Z.; Wolynes, P. G. *Annu. Rev. Phys. Chem.* **1997**, *48*, 545.
(6) Schuler, B.; Eaton, W. A. *Curr. Opin. Struct. Biol.* **2008**, *18*, 16.
(7) Ferguson, N.; Fersht, A. R. *Curr. Opin. Struct. Biol.* **2003**, *13*, 75.
(8) Ratner, V.; Amir, D.; Kahana, E.; Haas, E. *J. Mol. Biol.* **2005**, *352*, 683.
(9) Kimura, T.; Uzawa, T.; Ishimori, K.; Morishima, I.; Takahashi, S.; Konno, T.; Akiyama, S.; Fujisawa, T. *Proc. Natl. Acad. Sci. U.S.A.* **2005**, *102*, 2748.
(10) Roder, H. *Proc. Natl. Acad. Sci. U.S.A.* **2004**, *101*, 1793.
(11) Akiyama, S.; Takahashi, S.; Kimura, T.; Ishimori, K.; Morishima, I.; Nishikawa, Y.; Fujisawa, T. *Proc. Natl. Acad. Sci. U.S.A.* **2002**, *99*, 1329.
(12) Uzawa, T.; Akiyama, S.; Kimura, T.; Takahashi, S.; Ishimori, K.; Morishima, I.; Fujisawa, T. *Proc. Natl. Acad. Sci. U.S.A.* **2004**, *101*, 1171.
(13) Sinha, K. K.; Udgaonkar, J. B. *J. Mol. Biol.* **2007**, *370*, 385.
(14) Magg, C.; Kubelka, J.; Holtermann, G.; Haas, E.; Schmid, F. X. *J. Mol. Biol.* **2006**, *360*, 1067.
(15) Sinha, K. K.; Udgaonkar, J. B. *J. Mol. Biol.* **2005**, *353*, 704.
(16) Jennings, P. A.; Wright, P. E. *Science* **1993**, *262*, 892.
(17) Hagen, S. J.; Eaton, W. A. *J. Mol. Biol.* **2000**, *297*, 781.
(18) Shastry, M. C. R.; Roder, H. *Nat. Struct. Biol.* **1998**, *5*, 385.
(19) Parker, M. J.; Marqusee, S. *J. Mol. Biol.* **1999**, *293*, 1195.
(20) Hagen, S. J. *Proteins—Struct., Funct., Genetics* **2003**, *50*, 1.
(21) Qiu, L. L.; Zachariah, C.; Hagen, S. J. *Phys. Rev. Lett.* **2003**, *90*, 168103.
(22) Bilsel, O.; Matthews, C. R. *Curr. Opin. Struct. Biol.* **2006**, *16*, 86.
(23) Deniz, A. A.; Laurence, T. A.; Dahan, M.; Chemla, D. S.; Schultz, P. G.; Weiss, S. *Annu. Rev. Phys. Chem.* **2001**, *52*, 233.
(24) Deniz, A. A.; Laurence, T. A.; Beligere, G. S.; Dahan, M.; Martin, A. B.; Chemla, D. S.; Dawson, P. E.; Schultz, P. G.; Weiss, S. *Proc. Natl. Acad. Sci. U.S.A.* **2000**, *97*, 5179.
(25) Schuler, B.; Lipman, E. A.; Eaton, W. A. *Nature* **2002**, *419*, 743.
(26) Kuzmenkina, E. V.; Heyes, C. D.; Nienhaus, G. U. *Proc. Natl. Acad. Sci. U.S.A.* **2005**, *102*, 15471.
(27) Laurence, T. A.; Kong, X. X.; Jager, M.; Weiss, S. *Proc. Natl. Acad. Sci. U.S.A.* **2005**, *102*, 17348.
(28) Tezuka-Kawakami, T.; Gell, C.; Brockwell, D. J.; Radford, S. E.; Smith, D. A. *Biophys. J.* **2006**, *91*, L42.
(29) Sherman, E.; Haran, G. *Proc. Natl. Acad. Sci. U.S.A.* **2006**, *103*, 11539.
(30) Nettels, D.; Gopich, I. V.; Hoffmann, A.; Schuler, B. *Proc. Natl. Acad. Sci. U.S.A.* **2007**, *104*, 2655.
(31) Merchant, K. A.; Best, R. B.; Louis, J. M.; Gopich, I. V.; Eaton, W. A. *Proc. Natl. Acad. Sci. U.S.A.* **2007**, *104*, 1528.
(32) Hoffmann, A.; Kane, A.; Nettels, D.; Hertzog, D. E.; Baumgartel, P.; Lengefeld, J.; Reichardt, G.; Horsley, D. A.; Seckler, R.; Bakajin, O.; Schuler, B. *Proc. Natl. Acad. Sci. U.S.A.* **2007**, *104*, 105.
(33) Huang, F.; Sato, S.; Sharpe, T. D.; Ying, L. M.; Fersht, A. R. *Proc. Natl. Acad. Sci. U.S.A.* **2007**, *104*, 123.
(34) Hofmann, H.; Golbik, R. P.; Ott, M.; Hubner, C. G.; Ulbrich-Hofmann, R. *J. Mol. Biol.* **2008**, *376*, 597.
(35) Sherman, E.; Itkin, A.; Kuttner, Y. Y.; Rhoades, E.; Amir, D.; Haas, E.; Haran, G. *Biophys. J.* **2008**, *94*, 4819.
(36) Maki, K.; Cheng, H.; Dolgikh, D. A.; Roder, H. *J. Mol. Biol.* **2007**, *368*, 244.
(37) Shortle, D. *Faseb J.* **1996**, *10*, 27.
(38) Carra, J. H.; Privalov, P. L. *Faseb J.* **1996**, *10*, 67.
(39) Fuchs, S.; Cuatreca., P.; Anfinsen, C. B. *J. Biol. Chem.* **1967**, *242*, 4768.
(40) Zhang, H. J.; Huang, S.; Feng, Y. M.; Guo, P.; Jing, G. Z. *Arch. Biochem. Biophys.* **2005**, *441*, 123.
(41) Ellman, G. L. *Arch. Biochem. Biophys.* **1959**, *82*, 70.
(42) Nozaki, Y. *Methods Enzymol.* **1972**, *26*, 43.
(43) Bolen, D. W.; Santoro, M. M. *Biochemistry* **1988**, *27*, 8069.
(44) Lipman, E. A.; Schuler, B.; Bakajin, O.; Eaton, W. A. *Science* **2003**, *301*, 1233.
(45) Vámosi, G.; Gohlke, C.; Clegg, R. M. *Biophys. J.* **1996**, *71*, 972.
(46) Chen, H. M.; Chan, S. C.; Leung, K. W.; Wu, J. M.; Fang, H. J.; Tsong, T. Y. *Febs J.* **2005**, *272*, 3967.
(47) Krieger, F.; Fierz, B.; Bieri, O.; Drewello, M.; Kiefhaber, T. *J. Mol. Biol.* **2003**, *332*, 265.
(48) Neuweiler, H.; Schulz, A.; Bohmer, M.; Enderlein, J.; Sauer, M. *J. Am. Chem. Soc.* **2003**, *125*, 5324.
(49) Buscaglia, M.; Schuler, B.; Lapidus, L. J.; Eaton, W. A.; Hofrichter, J. *J. Mol. Biol.* **2003**, *332*, 9.
(50) Chow, C. Y.; Wu, M. C.; Fang, H. J.; Hu, C. K.; Chen, H. M.; Tsong, T. Y. *Proteins—Struct., Funct., Bioinf.* **2008**, *72*, 901.
(51) McCarney, E. R.; Werner, J. H.; Bernstein, S. L.; Ruczinski, I.; Makarov, D. E.; Goodwin, P. M.; Plaxco, K. W. *J. Mol. Biol.* **2005**, *352*, 672.
(52) Yang, M.; Liu, D.; Bolen, D. W. *Biochemistry* **1999**, *38*, 11216.
(53) Kohn, J. E.; Millett, I. S.; Jacob, J.; Zagrovic, B.; Dillon, T. M.; Cingel, N.; Dothager, R. S.; Seifert, S.; Thiyagarajan, P.; Sosnick, T. R.; Hasan, M. Z.; Pande, V. S.; Ruczinski, I.; Doniach, S.; Plaxco, K. W. *Proc. Natl. Acad. Sci. U.S.A.* **2004**, *101*, 12491.
(54) Tanford, C.; Kawahara, K.; Lapanje, S. *J. Biol. Chem.* **1966**, *241*, 1921.
(55) Miller, W. G.; Goebel, C. V. *Biochemistry* **1968**, *7*, 3925.
(56) Wrabl, J.; Shortle, D. *Nat. Struct. Biol.* **1999**, *6*, 876.
(57) Hyeon, C.; Dima, R. I.; Thirumalai, D. *J. Chem. Phys.* **2006**, *125*, 194905.
(58) Shortle, D.; Ackerman, M. S. *Science* **2001**, *293*, 487.
(59) Fitzkee, N. C.; Rose, G. D. *Proc. Natl. Acad. Sci. U.S.A.* **2004**, *101*, 12497.
(60) Wang, Y.; Shortle, D. *Biochemstry* **1995**, *34*, 15895.
(61) Chen, J.; Stites, W. E. *J. Mol. Biol.* **2004**, *344*, 271.
(62) Nishimura, C.; Riley, R.; Eastman, P.; Fink, A. L. *J. Mol. Biol.* **2000**, *299*, 1133.
(63) Arai, M.; Kondrashkina, E.; Kayatekin, C.; Matthews, C. R.; Iwakura, M.; Bilsel, O. *J. Mol. Biol.* **2007**, *368*, 219.

JP809825X